Physiology in Press; published online on August 3, 2006 as 10.1113/jphysiol.2006.115428

DIFFERENCES BETWEEN THE SCALING OF MINIATURE IPSCs AND EPSCs RECORDED IN THE DENDRITES OF CA1 MOUSE PYRAMIDAL NEURONS

Bertalan K. Andrásfalvy[1,*] *and Istvan Mody*[1,2]

[1]Institute of Experimental Medicine, Budapest, Hungary,
[2]Departments of Neurology and Physiology, UCLA, Los Angeles, CA, USA

/Distance dependence of mEPSCs and mIPSCs/

Key words: CA1, mEPSCs, mIPSCs

Number of pages: 19
Number of words: 2778

*To whom correspondences should be addressed.
Bertalan K. Andrásfalvy
Neuroscience Center, Louisiana State University Health Science Center,
2020 Gravier St.
New Orleans, LA 70112, USA
E-mail:bandra@lsuhsc.edu

Supported by NIH Grant NS 30549 and the Coelho Endowment to I. M.

Abstract

Anatomical studies have described inhibitory synaptic contacts on apical dendrites, and an abundant number of GABAergic synapses on the somata and proximal dendrites of CA1 pyramidal cells of the hippocampus (Megias et al, 2001). The number of inhibitory contacts decreases dramatically with distance from the soma, but the local electrophysiological characterization of these synapses at their site of origin in the dendrites is missing. We directly recorded dendritic GABA receptor-mediated inhibitory synaptic events in adult mouse hippocampal CA1 pyramidal neurons and compared them to excitatory synaptic currents recorded at the same sites.

Miniature GABAergic events were evoked using localized application of a hyperosmotic solution to the apical dendrites in the vicinity of the dendritic whole-cell recording pipette. Glutamatergic synaptic events were blocked by kynurenic acid, leaving picrotoxin-sensitive IPSCs. We measured the amplitude, and kinetic properties of mIPSCs at the soma and at three different dendritic locations. The amplitude of mIPSC recorded at the various sites was similar along the somato-dendritic axis. The rise and decay times of local mIPSC were also independent of the location of the synapses. The frequency of mIPSCs was 5 Hz at the soma, in contrast to <0.5 Hz at dendritic sites, which could be increased to 10-20 Hz and 6-10 Hz respectively by our hyperosmotic stimulation protocol.

Miniature glutamatergic events were evoked with the same protocol after blocking inhibitory synapses by bicucculine. The measured amplitudes increased along the somato-dendritic axis proportionally with their distance from the soma. The measured kinetic properties were independent of location.

Consistent with the idea that IPSCs may have a restricted local effect in the dendrites, our data show a lack of distance-dependent scaling of miniature inhibitory synaptic events, in contrast to the scaling of excitatory events recorded at the same sites.

Introduction

Integration of excitatory and inhibitory inputs determines neuronal firing. Hippocampal CA1 pyramidal neurons receive a number of GABAergic and glutamatergic afferents heterogeneously distributed along the somato-dendritic axis (Megias et al, 2001). Excitatory inputs from the Schaffer collaterals of CA3 pyramidal cells form synaptic connections on dendrites located in stratum radiatum and oriens, whereas the entorhinal cortex and some subcortical structures target distal apical dendrites in stratum lacunosum-moleculare through the perforant path (PP). The basal dendrites of CA1 pyramidal neurons are innervated by recurrent collaterals. Although different excitatory inputs arrive to spatially distinct parts of the dendritic tree, thus being differentially attenuated by the dendritic cable, electrophysiological experiments revealed that proximal and distal glutamatergic synaptic events in stratum radiatum have similar impact on neuronal output, independent of their spatial location (Magee & Cook, 2000). This phenomenon serves to increase synaptic efficacy with distance on the dendritic tree, and counterbalances the passive attenuation of synaptic events invading the soma (distance dependent scaling, Magee & Cook, 2000; Smith et al., 2003; Andrasfalvy et al., 2003).

Compared to excitatory inputs, distribution of inhibitory innervation of pyramidal neurons is more heterogeneous. Several distinct types of GABAergic interneuron innervate pyramidal cells, targeting different cellular compartments (Buhl, 1994; Halasy 1996, Somogyi & Klausberger 2005; Soltesz, 2005). Basket cells innervate the somata and proximal dendrites, axo-axonic cells target the initial segment of the axon, whereas distal dendrites are innervated by oriens-

lacunosum-moleculare (O-LM) interneurons. Anatomical and electrophysiological studies suggest that different inhibitory neurons have distinct roles in synaptic integration (Freund & Buzsaki, 1996; Klausberger et al., 2001; Somogyi & Klausberger 2005). The effects of certain interneuron classes on their targets depend on subcellular orientation of their connections, electrical properties of synaptic transmission and the actual postsynaptic membrane potential influenced by postsynaptic voltage-dependent ion channels.

Although detailed anatomical studies and electrophysiological works using somatic recording examined interneuron-pyramidal cell interactions (Pearce 1993; Buhl et al., 1996; Freund & Buzsaki, 1996; Hajos & Mody, 1997; Ouardouz & Lacaille, 1997; Klausberger et al., 2001; Somogyi & Klausberger 2005), recordings of local GABAergic synaptic events along the dendritic arborisation have rarely been done (Cossart et al, 2000; Dinocourt et al., 2003). In order to characterize local dendritic inhibitory synaptic events and to compare them to excitatory events, in this study we systematically investigated properties of locally evoked IPSCs recorded along the main shaft of apical dendrites of CA1 pyramidal cells.

Methods

Slice preparation and maintenance

All experiments were carried out according to methods approved by the Experimental Medicine Institutional Animal Care and Use Committee. Briefly, 42-90 day-old mice (C57BL6) were decapitated and the brains dissected and placed in cold oxygenated low-Ca^{2+}/high-Mg^{2+}slicing solution. Hippocampal slices (350 µm) were prepared using previously described standard procedures (Magee & Cook, 2000). Three dendritic regions were examined, namely 1) a proximal recording location 50-80 µm from the soma (where dendritic spine density becomes substantial), 2) a middle location: 100-120 µm from the soma and 3) a distal location: 180-220 µm from the soma, situated about 20 µm from the border of stratum radiatum and lacunosum-moleculare. Somatic recordings of mIPSCs were also performed, to focus on the highest density of inhibitory input region according to anatomical studies (Megias et al, 2001). Experiments were conducted using an upright Ziess Axioskope microscope equipped with differential interference contrast (DIC) optics using infrared illumination. For the measurement of mEPSCs and mIPSCs, patch pipettes (5-8 MΩ) were pulled from borosilicate glass and filled with one of the the following internal solutions: for mEPSCs (containing in mM) 120 Cs-gluconate, 20 $CsCl_2$, 0.5 EGTA, 4 NaCl, 0.3 $CaCl_2$, 4 Mg_2ATP, 0.3 $Tris_2GTP$, 14 phosphocreatine and 10 HEPES (pH 7.2), and for mIPSCs (in mM) 60 Cs-gluconate, 80 $CsCl_2$, 0.5 EGTA, 4 NaCl, 0.3 $CaCl_2$, 4 Mg_2ATP, 0.3 $Tris_2GTP$, 14 phosphocreatine and 10 HEPES (pH 7.2). The external solution contained 125 mM NaCl, 2.5 mM KCl, 1.25 mM NaH_2PO_4, 25 mM $NaHCO_3$, 2 mM $CaCl_2$, 2 mM $MgCl_2$, 25 mM dextrose and 0.5 mM tetrodotoxin TTX), bubbled with 95% O_2 and 5% CO_2 at room temperature (pH

7.4). All neurons had resting potentials between -60 and –75 mV. Series resistances of dendritic whole-cell recordings were between 10 and 30 MΩ. Miniature synaptic events were evoked by pressure ejection of a hyperosmotic (~600 mosm) external solution (**see Fig. 1**) containing +300 mM sucrose and HEPES (10 mM) replacing $NaHCO_3$. Synaptic events were collected between 1 and 5 s following pressure ejection of the hyperosmotic solution. AMPA receptor currents were isolated by the presence of external $MgCl_2$ (2 mM) and (+)-bicuculline (10 mM). GABAA receptor currents were recorded in the presence of external kynurenic acid (3 mM). Currents were recorded at –70 mV using a MultiClamp 700A amplifier (Axon Instruments), filtered at 2 kHz and digitized at 10 kHz. Each recording was made from different cells. All experiments were conducted at room temperature.

Data analysis

Recordings were analyzed using a LabView-based in-house event detection and analysis (EVAN) software package (www.EVAN.Thotec.com). Events were fitted with a sum of two exponential functions to obtain peak amplitude, rise-time (20 to 80% of peak amplitude) and decay-time ($T_{50decay}$) constants. Analysis was performed only on recordings where the mean rise time (20 to 80% of peak amplitude) of the mEPSCs or mIPSCs was < 1 ms. In previous studies performed at 33-34 ˚C, events with 400 μs rise time (tau of exponential fit) constants or less were examined only, since slower events were unlikely to be local (Magee & Cook, 2000). In our present study at room temperature we used wider time range, because of the temperature dependence of kinetic properties of miniature synaptic currents. Miniature EPSCs and IPSCs larger than the ~4 pA threshold level were

detected. Cumulative frequency plots were generated from 50 randomly picked events (at all indicated location) from 3 cells each.

All experimental values are presented as mean ± S.E.M. Statistical significance ($p<0.05$) was determined with one-way ANOVA and post hoc analysis with Tukey's honest significance difference test (Statistica).

Results

Local recording of glutamatergic synaptic events

Whole-cell recordings from different spiny regions of the apical dendritic arbor were used to record miniature excitatory postsynaptic currents (mEPSCs) (Andrasfalvy *et al*. 2003). Synaptic events were recorded at proximal apical dendrites (50-80 μm from soma), at middle location (100-120 μm) and at distal location of stratum radiatum (180-220 μm from soma) of mouse hippocampal CA1 pyramidal neurons (**Fig. 1**). The examined region of apical dendrites represents the spiny part of stratum radiatum, where the Schaffer collaterals are the sole excitatory inputs. Somatic recording of glutamatergic events was excluded, based on anatomical observations indicating that the soma and the first ~50 μm of proximal dendrites lack spines. Besides analyzing the properties of spontaneously occurring mEPSCs, we also used local pressure ejection of a hyperosmotic external solution to stimulate release of synaptic vesicles (evoked mEPSCs; see Methods and **Fig. 1**; Magee & Cook, 2000; Andrasfalvy *et al*. 2003; Smith *et al.* 2003).

The frequency of spontaneously occurring miniature synaptic AMPA currents was found to be similar at all three recording sites on apical dendrites (**Fig. 2A and 4A**; at ~50 μm: 0.74 ± 0.36 Hz, n=5; at ~120 μm: 0.28 ± 0.10 Hz, n=4; at

~200 μm: 0.50 ± 0.22 Hz, n=6, p>0.5, ANOVA). Frequency of evoked mEPSCs was also similar at different locations (at ~50 μm: 6.50 ± 0.99 Hz; at ~120 μm: 9.54 ± 3.41 Hz; at ~200 μm: 9.35 ± 1.18 Hz, p>0.2).

Consistent with data obtained from rats and mice at 33-34 ˚C (Magee & Cook, 2000; Smith *et al.* 2003; Andrasfalvy *et al*. 2003), mEPSC amplitudes recorded in mice at room temperature increased continuously with distance ($p<0.01$, ANOVA), and distal events were approximately 1.5-fold larger than proximal events (**Fig. 4B**; at ~50 μm: 14.71 ± 1.62 pA, n=5; at ~120 μm: 16.82 ± 1.46 pA, n=4; at ~200 μm: 23.26 ± 1.64 pA, n=6). Cumulative frequency distributions (Fig. 2B) demonstrate, also that distal synaptic inputs are uniformly shifted towards larger amplitudes,

Kinetic properties of synaptic AMPA currents were also similar regardless of dendritic location (**Fig. 4G**; $T_{rise20/80}$: at ~50 μm: 439 ± 58 μs; at ~120 μm: 408 ± 49 μs; at ~200 μm: 432 ± 35 μs; p>0.8; **Fig. 4H** $T_{50decay}$: at ~50 μm: 4.76 ± 0.34 ms; at ~120 μm: 4.61 ± 0.57 ms; at ~200 μm: 4.27 ± 0.28 ms; p>0.8).

Local recording of GABAergic synaptic events

After confirming that distance-dependent scaling of mEPSCs was similar to that previously established (Magee & Cook, 2000; Andrasfalvy *et al*. 2003; Smith *et al.* 2003), we next examined whether electrophysiological properties of mIPSCs also show distance-dependent alterations. Somatic and proximal apical dendrites represent approximately ~40% of symmetrical synapses (Megias et al., 2001), originating mostly from basket cells. Further away, the density GABAergic

synapses drastically decreases on apical dendrites; these synapses are formed by bistratified, CCK basket, radial and horizontal trilaminar cells (Freund & Buzsaki, 1996; Buhl et al., 1996; Megias et al., 2001; Klausberger et al., 2002). Because inhibitory synapses heavily innervate not only the dendrites but also the somata of CA1 pyramidal cells, somatic recordings were also performed in the case of mIPSCs.

Frequency of spontaneously occurring mIPSCs was high at the soma (**Fig. 3;** 5.36 ± 0.66 Hz, n=13, $p<0.005$), whereas activity dramatically decreased on dendrites, already at the proximal recording site (at 50 μm: 0.91 ± 0.35 Hz, n=5; at ~120 μm: 0.71 ± 0.31 Hz, n=7; at ~200 μm: 0.91 ± 0.37 Hz, n=8). Frequency of evoked synaptic $GABA_A$ receptor-mediated currents was not significantly different between the different recording locations (**Fig. 3A and 4C**; soma: 13.16 ± 4.39 Hz; at ~50 μm: 7.37 ± 1.35 Hz; at ~120 μm: 9.25 ± 1.39 Hz; at ~200 μm: 9.05 ± 2.63 Hz, $p>0.5$). The high spontaneous somatic mIPSC activity was not detected at dendritic recordings, even at the closest (~50 μm) location, suggesting that the high somatic activity may represent a technical artifact of somatic patching or that it may be disproportionately attenuated by the short dendritic segment.

Importantly, we found that the amplitude of hyperosmotic solution evoked GABAergic synaptic events was similar at every recording location along the apical dendrite (**Fig. 4D**; soma: 14.6 ± 1.5 pA, n=13; at ~50 μm: 15.3 ± 1.8 pA, n=5; at ~120 μm: 14.4 ± 1.5 pA, n=7; at ~200 μm: 17.85 ± 2.1 pA, n=8, $p>0.5$), indicating that, in contrast to excitatory AMPA receptor-mediated currents, inhibitory $GABA_A$ receptor-mediated synaptic events do not exhibit distance-dependent increase of amplitudes. Cumulative frequency distributions (Fig. 3B)

from different location almost overlap each other, even the most distal events amplitudes shifts is not significant.

Kinetic properties of synaptic GABA currents were also similar at different recording sites (**Fig. 4I, J**; $T_{rise20/80}$: soma: 501 ± 20 μs; at ~50 μm: 442 ± 34 μs; at ~120μm: 481 ± 32 μs; at ~200 μm: 504 ± 43 μs, p>0.5; $T_{50decay}$: soma: 7.4 ± 0.3 ms; at ~50 μm: 7.1 ± 0.6 ms; at ~120 μm: 6.6 ± 0.4 ms; at ~200 μm: 6.1 ±0 .3 ms, p>0.1).

Discussion

In this study we have systematically characterized the properties of synaptic inhibitory and excitatory currents recorded in adult mice locally in the soma and in the apical dendrites all the way to the border of stratum radiatum. Using local somatic or dendritic whole-cell voltage-clamp recordings, we examined spontaneous events as well as currents evoked by application of hyperosmotic solution in hippocampal CA1 pyramidal neurons,.

The most important finding of our study is that, while excitatory synapses show distance-dependent scaling, inhibitory synaptic currents exhibit similar amplitude and kinetic properties along the dendritic tree. The lack of a counter balancing mechanism alleviating the effects of dendritic cable attenuation for $GABA_A$ receptor-mediated synaptic currents is consistent with the main role of

dendritic inhibitory synapses; i.e., the precise control of local excitatory conductances to adjusting their impact on somatic output. In contrast, distance-dependent scaling of excitatory synaptic events ensures that these synapses can have the same impact on the soma, regardless of their remote location.

We also found that the frequency of spontaneous synaptic GABA receptor currents at the somatic region was significantly higher than further away from soma, whereas the frequency of evoked synaptic GABA receptor currents did not differ between different dendritic locations. Kinetic properties of synaptic GABA currents were similar everywhere, similar to AMPA receptor-mediated currents that did not show kinetic differences along the dendrites. In our experiments the high spontaneous somatic mIPSC activity was not present at nearby (~50 μm) dendritic recordings, suggesting that the close location of the recording pipettes to the highest density of inhibitory terminals (soma, soma-neck) during somatic patching may enhance GABA release.

Cossart et al., 2000, showed decreased dendritic mIPSCs compared to somatic mIPSCs. Their dendritic data included recordings 120-480 μm away from the soma, raising the possibility that anatomically heterogeneous inputs (Megias et al., 2001) might have been lumped together. In addition, the spatial origins of the events were not controlled and the wide rise time criteria used in their study allowed the inclusion of remotely generated events into the analysis

Previous studies describing fast and slow synaptic $GABA_A$–receptor mediated events, have focused on two anatomical distinct regions (stratum lacunosum-moleculare and stratum radiatum) of CA1 pyramidal neurons (Pearce, 1993; Pouille & Scanziani, 2004). Several recent studies (Glykys and Mody, 2006; Prenosil et al. 2006) have come to the conclusion that the slow GABAergic

spontaneous events originally described by Pearce might be generated by overspill. In the presence of TTX, the likelihood of overspill is reduced, thus the lack of slow events in our recordings.

Several experimental and theoretical studies (Miles et al, 1996; Cossart et al, 2000; Yang et al, 2003) also support the idea, that spatially distributed inhibitory events have different effects on postsynaptic cell activity and these events have mostly local impact. However, recently published findings, support possible excitatory roles of GABAergic events on pyramidal neurons (Gulledge & Stuart, 2003; Szabadics et al., 2006). The excitatory role of GABAergic inputs depends on their spatiotemporal relationship to other depolarizing events (Gulledge & Stuart, 2003) and on locally increased intracellular Cl^- concentrations possibly resulting from Cl^- transporter density differences between the axo-somato-dendritic axis (Szabadics et al., 2006). Nevertheless, the lack of distance-dependent scaling of dentritic GABA synapses found in our study is consistent with their main role as controlling the effectiveness of local excitatory conductances.

References

Andrasfalvy BK & Magee JC (2001) Distance-dependent increase in AMPA receptor number in the dendrites of adult hippocampal CA1 pyramidal neurons. *J Neurosci* **21**, 9151–9159.

Andrasfalvy BK, Smith MA, Borchardt T, Sprengel R, Magee JC. (2003) Impaired egulation of synaptic strength in hippocampal neurons from GluR1-deficient mice. *J Physiol.* **552**, 35-45.

Buhl E. H., Halasy K. and Somogyi P. (1994) Diverse sources of hippocampal unitary inhibitory postsynaptic potentials and the number of synaptic release sites. *Nature* **368,** 823–828.

Cossart R, Hirsch JC, Cannon RC, Dinoncourt C, Wheal HV, Ben-Ari Y, Esclapez M, Bernard C. (2000) Distribution of spontaneous currents along the somato-dendritic axis of rat hippocampal CA1 pyramidal neurons. *Neuroscience*. **99**, 593-603.

Cossart R, Dinocourt C, Hirsch JC, Merchan-Perez A, De Felipe J, Ben-Ari Y, Esclapez M, Bernard C (2001) Dendritic but not somatic GABAergic inhibition is decreased in experimental epilepsy. *Nat Neurosci* **4**, 52–62

Dinocourt C, Petanjek Z, Freund TF, Ben-Ari Y, Esclapez M. (2003) Loss of interneurons innervating pyramidal cell dendrites and axon initial segments in the CA1 region of the hippocampus following pilocarpine-induced seizures. J Comp *Neurol.* **459**, 407-25

Freund, T. F. & Buzsa´ki, G. (1996) Interneurons of the hippocampus. Hippocampus 6, 347–470

Glykys J, Mody I. (2006) Hippocampal network hyperactivity after selective reduction of tonic inhibition in GABA A receptor alpha5 subunit-deficient mice. *J Neurophysiol*. **95**, 2796-807.

Gulledge AT, Stuart GJ. (2003) Excitatory actions of GABA in the cortex. *Neuron*. **37**, 299-309.

Hajos N & Mody I. (1997) Synaptic communication among hippocampal interneurons: properties of spontaneous IPSCs in morphologically identified cells. *J Neurosci*. **17**, 8427-42.

Klausberger T, Roberts JD, Somogyi P. (2002) Cell type- and input-specific differences in the number and subtypes of synaptic GABA(A) receptors in the hippocampus. J Neurosci. **22**: 2513-21.

Magee JC & Cook EP. (2000) Somatic EPSP amplitude is independent of synapse location in hippocampal pyramidal neurons. *Nat Neurosci* **3**, 895–903.

Magee JC (2000) Dendritic integration of excitation synaptic input. *Nat Rev Neurosci* **1**, 181–190.

Megias M, Emri Z, Freund TF, Gulyas AI. (2001) Total number and distribution of inhibitory and excitatory synapses on hippocampal CA1 pyramidal cells. *Neurosci*. **102**: 527-540

Miles R, Toth K, Gulyas AI, Hajos N, Freund TF. (1996) Differences between somatic and dendritic inhibition in the hippocampus. *Neuron*. **16**, 815-23

Mody I. & Pearce RA. (2004) Diversity of inhibitory neurotransmission through GABA(A) receptors. *Trends Neurosci.* **27**, 569-75. Review.

Ouardouz M, Lacaille JC. (1997) Properties of unitary IPSCs in hippocampal pyramidal cells originating from different types of interneurons in young rats. *J Neurophysiol*. **77**, 1939-49.

Pearce, R.A. (1993) Physiological evidence for two distinct GABAA responses in rat hippocampus. Neuron *10*, 189–201.

Pouille F, Scanziani M. (2004) Routing of spike series by dynamic circuits in the hippocampus. *Nature* **429**,717-723.

Prenosil GA, Schneider Gasser EM, Rudolph U, Keist R, Fritschy JM, Vogt KE. (2006) Specific Subtypes of GABAA Receptors Mediate Phasic and Tonic Forms of Inhibition in Hippocampal Pyramidal Neurons. *J Neurophysiol*. **96**, 846-57.

Smith MA, Ellis-Davies GCR & Magee JC (2003) Mechanism of the distance-dependent scaling of Schaffer collateral synapses in rat CA1 pyramidal neurons. *J Physiol* **548**, 245–258.

Soltesz I. (2006) *Diversity in the Neuronal Machine*. Oxford University Press,

238 pp.

Somogyi P, Klausberger T. (2005) Defined types of cortical interneurone structure space and spike timing in the hippocampus. *J Physiol*. **562**, 9-26. Review.

Spruston, N., Jaffe, D. B., Williams, S. H. & Johnston, D. (1993) Voltage- and space-clamp errors associated with the measurement of electrotonically remote synaptic events. *J. Neurophysiol*. **70**, 781–802.

Szabadics J, Varga C, Molnar G, Olah S, Barzo P, Tamas G. (2006) Excitatory effect of GABAergic axo-axonic cells in cortical microcircuits. *Science*. **311**, 233-5.

Tamas G., Szabadics J., Lorincz A. and Somogyi P. (2004) Input and frequency-specific entrainment of postsynaptic firing by IPSPs of perisomatic or dendritic origin. *Eur. J. Neurosci*. **20,** 2681–2690.

Yang KH, Franaszczuk PJ, Bergey GK. (2003) The influences of somatic and dendritic inhibition on bursting patterns in a neuronal circuit model. *Biol Cybern*. **89**, 242-53.

Acknowledgements

We are thankful for the assistance of Ferenc Mátyás in anatomical reconstruction.

Figures and legend

Figure 1. Anatomy of a mouse CA1 pyramdial neuron and schematic view of the used recording protocol.

Left, morphology of a typical recorded CA1 pyramidal cell filled with BDA. Right, schematic diagram of the stimulation and recording sites in CA1 pyramidal cells using the whole-cell dendritic voltage-clamp (VC) technique, combined with local stimulation of synapses by ejecting hyperosmotic external solution. (Scale bar indicates 100 μm.)

Figure 2. Representative recording of mEPSCs.

A, Representative traces of spontaneous (left, grey) and hypertonic solution-evoked (right, black) mEPSCs from proximal (~50 μm), middle (~120 μm) and distal (~200 μm) apical dendrites of an adult mouse CA1 pyramidal cell. The amplitude of evoked mEPSCs increased with distance from soma. B, Cumulative distribution of 50-50 miniature events of 3-3 cells at 3 different locations on apical dendrites.

Figure 3. Representative recording of mIPSCs.

A, Representative traces of spontaneous (left, grey) and hypertonic solution-evoked (right, black) mIPSCs from proximal (~50 μm), middle (~120 μm) and distal (~200 μm) apical dendrites as well as from soma of an adult mouse CA1 pyramidal cell. The amplitude of evoked mIPSCs did not change with distance from soma. Note the high spontaneous mIPSC activity at the somatic recording. **B**, Cumulative distribution of 50-50 miniature events of 3-3 cells at soma and 3 different locations on apical dendrites.

Figure 4. Summary of electrophysiological properties of spontaneous and osmotically evoked mEPSCs (A, B) and mIPSCs (C, D) recorded at different dendritic distances. A and **C,** amplitude of evoked miniature events. **B** and **D,** frequency of spontaneous (grey columns) and evoked (black columns) events. **G** and **I**, 20-80% rise time, **H** and **J**, 50 % decay time of evoked events. Middle panels (**E, F**) show single representative miniature currents recorded at different locations. (*, ** and *** indicates $p<0.05$, $p<0.01$ and $p<0.005$, respectively)

Figure 1

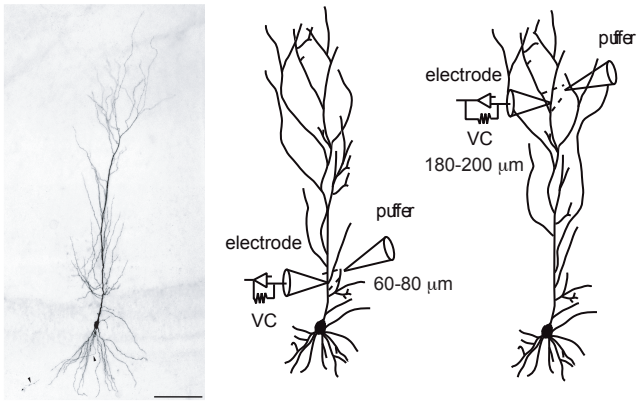

Figure 2

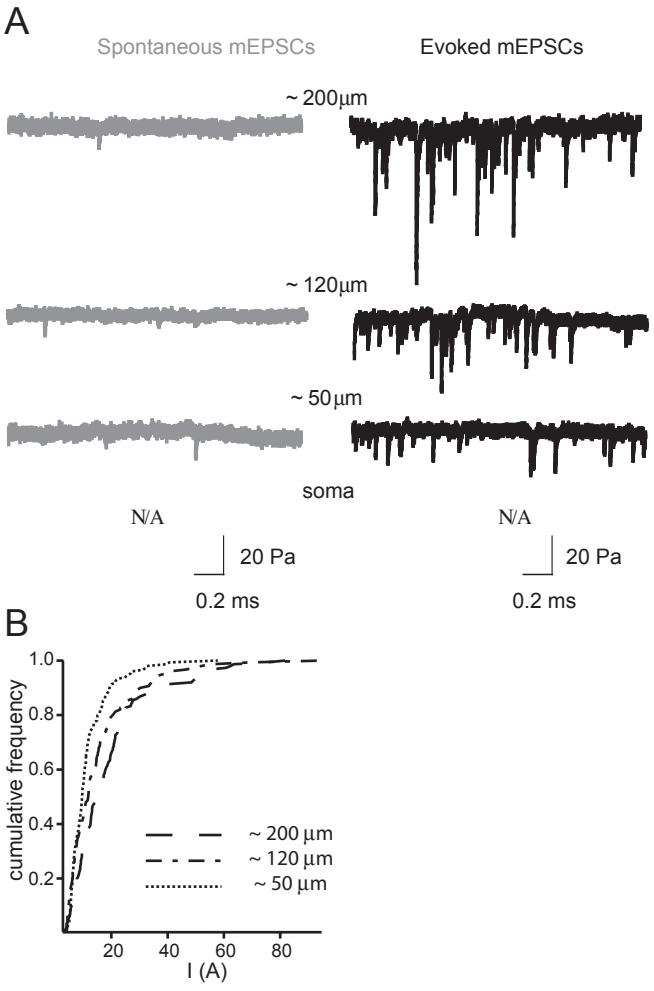
A
Spontaneous mEPSCs
Evoked mEPSCs
~ 200µm
~ 120µm
~ 50µm
soma
N/A
N/A
20 Pa
20 Pa
0.2 ms
0.2 ms
B
cumulative frequency
1.0
0.8
0.6
0.4
0.2
20
40
60
80
I (A)
~ 200 µm
~ 120 µm
~ 50 µm

Figure 3

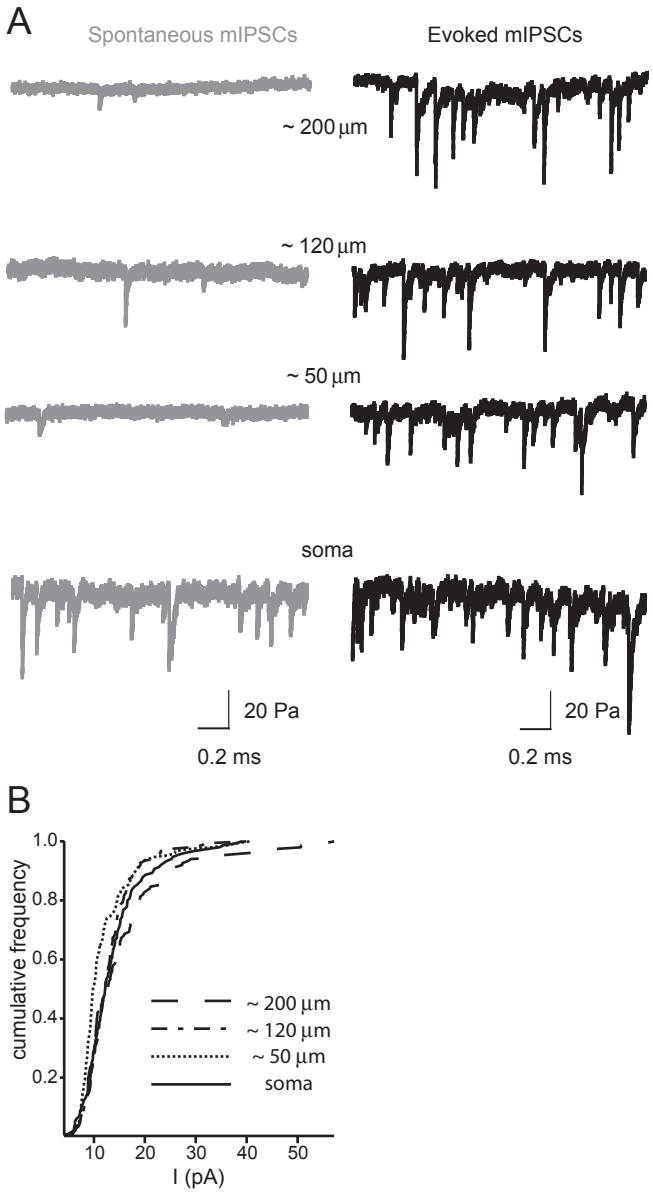
A
Spontaneous mIPSCs
Evoked mIPSCs
~ 200 µm
~ 120 µm
~ 50 µm
soma
20 Pa
0.2 ms
20 Pa
0.2 ms
B
cumulative frequency
1.0
0.8
0.6
0.4
0.2
10
20
30
40
50
I (pA)
~ 200 µm
~ 120 µm
~ 50 µm
soma

Figure 4

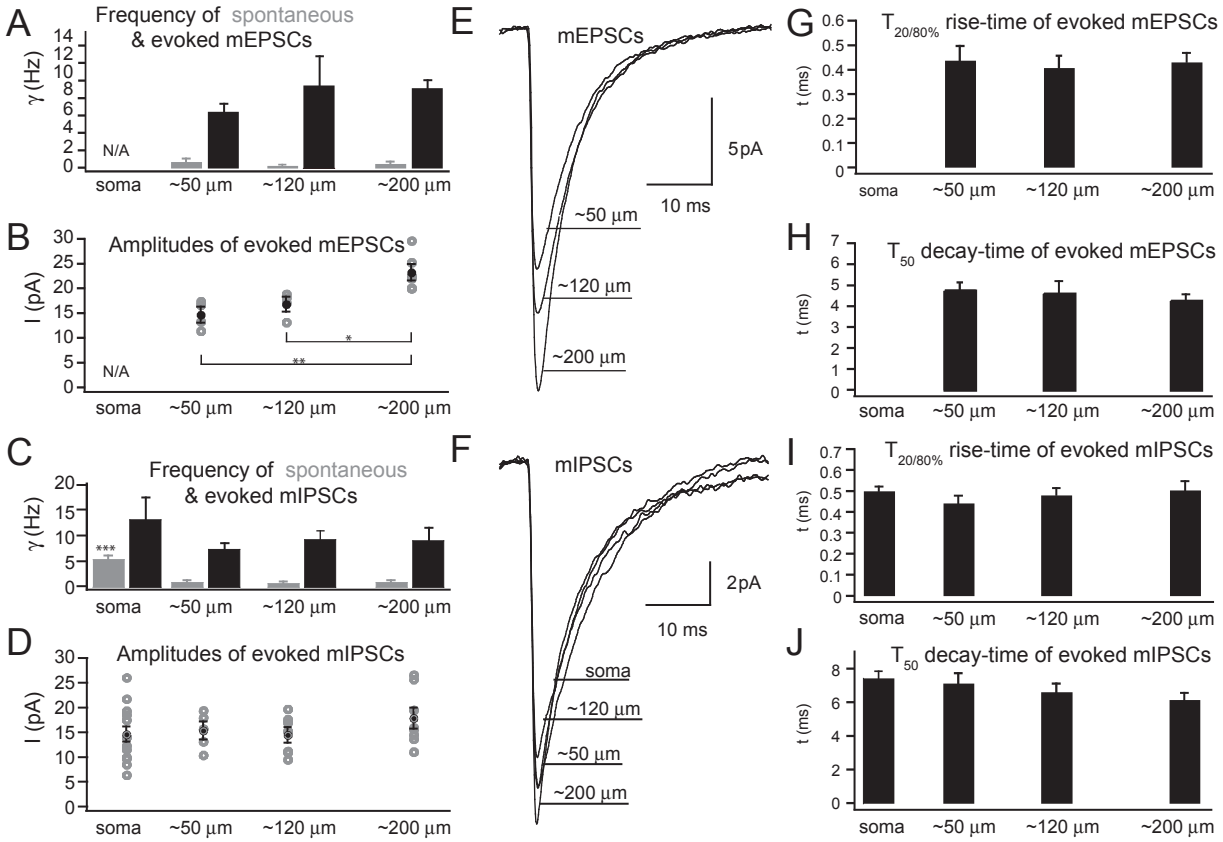
A
Frequency of spontaneous & evoked mEPSCs
γ (Hz)
N/A
soma
~50 µm
~120 µm
~200 µm
B
Amplitudes of evoked mEPSCs
I (pA)
N/A
*
**
C
Frequency of spontaneous & evoked mIPSCs
***
D
Amplitudes of evoked mIPSCs
E
mEPSCs
5pA
10 ms
F
mIPSCs
2pA
G
T20/80% rise-time of evoked mEPSCs
t (ms)
H
T50 decay-time of evoked mEPSCs
I
T20/80% rise-time of evoked mIPSCs
J
T50 decay-time of evoked mIPSCs